Analytical Two-Degrees-of-Freedom (2-DOF) Decoupling Control Scheme for Multiple-Input−Multiple-Output (MIMO) Processes with Time Delays

Tao Liu* and Weidong Zhang

Department of Automation, Shanghai Jiaotong University, Shanghai 200240, People's Republic of China

Furong Gao

Department of Chemical Engineering, Hong Kong University of Science & Technology, Clear Water Bay, Kowloon, Hong Kong

A two-degrees-of-freedom (2-DOF) decoupling control scheme is proposed for multiple-input−multiple-output (MIMO) processes with time delays. The set-point response and load-disturbance response of each process output can be separately regulated and optimized online. The two respective controller matrices for set-point tracking and load-disturbance rejection are analytically derived based on the H_2 optimal performance specification and rational transfer function approximation. A simplified stability condition is given to check the resulting control system stability, together with a graphical approach, in terms of the multivariable spectral radius stability criterion, to evaluate the robust stability of the control system in the presence of the process additive and multiplicative uncertainties. Correspondingly, an on-line tuning rule for the adjustable parameters of the two controller matrices is given to accommodate the unmodeled process dynamics. Finally, illustrative examples are given to demonstrate the merits of the proposed 2-DOF decoupling control scheme.

1. Introduction

Control of multiple-input−multiple-output (MIMO) systems remains a challenge in the process control community, in particular for those processes with time delays. Many MIMO control systems are tuned conservatively in practice to guarantee system stability. Such practices inevitably result in undesirable interactions among individual control loops, leading to poor system performance and waste of materials and energy.[1,2] For MIMO control system design, it is common to model the process in the form of a transfer matrix. Both simultaneous and sequential relay feedback methods have been developed to obtain transfer matrix models of MIMO processes (see, e.g., refs 3−10). Early literature[11−13] discussed performance limitations on the process dynamic resilience in the presence of right-half-plane (RHP) zeros and time delays. A few control bibliographies[14−16] studied the effect of model uncertainty on the process dynamic resilience. According to the internal model control (IMC) principle,[14] Jerome and Ray[17] presented a decoupling controller matrix design using a geometrical diagram approach for MIMO systems with time delays. This was followed by improved tuning methods that were developed in refs 18 and 19. Based on the multivariable Smith predictor control structure,[20] refs 21 and 22 proposed tuning methods in terms of frequency response specifications, such as the ultimate frequency and the magnitude/phase margins. By specifying the closed-loop system transfer matrix with a desirable frequency response characteristic, Wang et al.[23] presented an enhanced tuning of decoupling controller matrix within the framework of a conventional unity feedback control structure. This recently was further improved for implementation and performance by Liu et al.[24] Many decoupling control methods have been developed using a decoupler in front of the process inputs to realize diagonal dominance of the augmented process transfer matrix, such as those described in refs 25−27, which are based on a dynamic decoupler, and those described in refs 28−30, which are based on a static decoupler (i.e., the inverse of the process static gain transfer matrix). However, note that a dynamic decoupler is actually difficult to be configured precisely, especially for MIMO processes with high dimension or large time delays.[25,30] In contrast, a static decoupler has no impact on dynamic decoupling for the augmented process. Besides, it should be mentioned that, although the recently developed decentralized/mutiloop control methods (see, e.g., refs 31−34) are capable of remarkably improved output performance, when compared to many existing methods, tuning of these decentralized controllers is confined to a tradeoff between the achievable system output performance and the interaction level among individual loops.

Note that most existing decoupling control methods, including the aforementioned literature, perform set-point tracking and load-disturbance rejection via a single controller matrix or a set of decentralized controllers in series with a static/dynamic decoupler. Set-point tracking and load-disturbance rejection cannot be separately regulated or optimized. Although two-degrees-of-freedom (2-DOF) control methods have been reported in the literature,[35−37] using weighting functions and H_∞ norm optimization approaches, an integrated controller matrix was derived eventually for both set-point tracking and load-disturbance rejection. Therefore, these methods cannot be utilized to regulate set-point tracking and load disturbance rejection separately online.

Recently, Huang et al.[38] proposed a new 2-DOF decoupling control structure with obviously improved performance for load disturbance rejection, whereas there exist more than two controller matrices tuned by numerical iteration algorithms, which involve considerable computation effort for implementation and on-line tuning. Therefore, a simplified 2-DOF decoupling control structure is proposed in this paper. Both set-point tracking and load-disturbance rejection for each process output can be separately regulated and optimized online, while significant or even absolute decoupling regulation performance

* To whom correspondence should be addressed. Tel/Fax: +86.21.34202019. E-mail address: liurouter@ieee.org.

10.1021/ie0612921 CCC: $37.00
Published on Web 08/30/2007

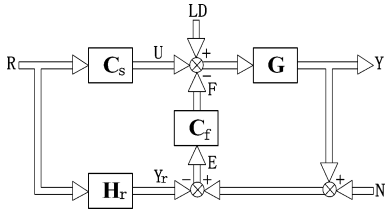

Figure 1. Multivariable two-degrees-of-freedom (2-DOF) decoupling control structure.

can be achieved. The computation effort can be reduced significantly using the analytical controller design procedure recently developed in refs 19 and 24. The controllers of each column in the set-point tracking controller matrix are tuned in common by a single adjustable parameter. In a similar way, the controllers of each row in the closed-loop controller matrix for load disturbance rejection are tuned in common by a different single adjustable parameter. These merits can greatly facilitate operation of the system in practice. The paper is organized as follows: Section 2 presents the proposed 2-DOF decoupling control structure. In section 3, the practically desired diagonal system transfer matrices for set-point tracking and load-disturbance rejection are formulated according to the implementation constraints and H_2 optimal performance objective. Thereby, the desired set-point tracking controller matrix and closed-loop controller matrix for load-disturbance rejection, together with their executable forms, are derived analytically in section 4. In section 5, a simplified stability condition is presented to evaluate the nominal stability of the resulting control system, together with the multivariable spectral radius stability criterion for assessment of the control system robust stability. Correspondingly, an on-line tuning rule for the adjustable parameters in the two controller matrices is given to accommodate the unmodeled process dynamics in practice. Illustrative examples are included in section 6, to demonstrate the merits of the proposed 2-DOF decoupling control scheme. Finally, conclusions are presented in section 7.

2. New Multivariable 2-DOF Decoupling Control Structure

The proposed 2-DOF decoupling control structure for a MIMO process with time delays is shown in Figure 1, where G is the multivariable process to be regulated, which is generally modeled in the form of

$$G = \begin{bmatrix} g_{11} & \cdots & g_{1m} \\ \vdots & \ddots & \vdots \\ g_{m1} & \cdots & g_{mm} \end{bmatrix} \tag{1}$$

where $g_{ij}(s) = g_{0,ij}(s)e^{-\theta_{ij}s}$ (for $i, j = 1, 2, ..., m$), of which $g_{0,ij}(s)$ is a delay-free, physically proper, and stable transfer function. $C_s = [c_{ij}]_{m\times m}$ is the set-point tracking controller matrix. $H_r = \mathrm{diag}[h_{r,i}]_{m\times m}$ is a diagonal system transfer matrix for yielding decoupled reference output responses $Y_r = [y_{r,i}]_{m\times 1}$. The controller matrix $C_f = [cf_{ij}]_{m\times m}$, installed in the feedback channels of the closed-loop structure set between the process inputs and outputs, is utilized for rejecting load disturbances and eliminating the system output errors. The load disturbances are denoted by $\mathrm{LD} = [d_i]_{m\times 1}$ and the system output measurement noises are denoted as $N = [n_i]_{m\times 1}$.

Figure 1 shows that single feed-forward control for the set-point tracking is realizable if

$$H_r = GC_s \tag{2}$$

Note that, without model mismatch, the system output error signal ($E = [e_i]_{m\times 1}$) is zero if no load disturbance (LD) or measurement noise (N) exists. With the existence of load disturbances and/or measurement noises, the error signal (E) will no longer be zero and, thus, trigger the closed-loop controller matrix C_f to regulate the process inputs for counterbalance.

Hence, the proposed 2-DOF control structure allows independent design and regulation for set-point tracking and load-disturbance rejection. Given that H_r is adopted for yielding referential output responses, it may be viewed as a frequency-domain model predictive control (MPC) strategy for the set-point tracking. To implement decoupling regulation, the controller matrices C_s and C_f should be designed respectively to realize diagonal transfer matrix forms for the set-point response and the load-disturbance response. Considering that the achievable system performance for a MIMO process with time delays is constrained by the time delays of individual channels and possible non-minimum-phase (NMP) characteristics,[11−13] we prefer to have a discussion on the desired forms for set-point tracking and load disturbance rejection before proceeding with the derivation of C_s and C_f.

Remark 1. Note that MIMO processes with a nonsingular static gain transfer matrix (i.e. $\det[G(0)] \neq 0$) are studied in this paper. That is to say, each of the output responses are expected to be decoupled from each other.[2] It is true that, although some industrial processes can be modeled in the stable form of eq 1, their inverse transforms are sensitive to the process uncertainties. The reason lies in $\det[G(0)] \to 0$ for such a case. Therefore, such process modeling should be avoided for decoupling control design, for example, by changing the pairing for regulation between the process inputs and outputs. Note that, by constructing the square form of eq 1 between the process outputs to be decoupled and the process inputs, the proposed 2-DOF control scheme may be applied, in practice, to nonsquare systems.

◇

3. Desired Transfer Matrices for 2-DOF Control

From eq 2, the set-point tracking controller matrix can be derived as

$$C_s = G^{-1}H_r = \frac{\mathrm{adj}(G)}{\det(G)}H_r \tag{3}$$

where $\mathrm{adj}(G) = [G^{ij}]^{\mathrm{T}}_{m\times m}$ is the adjoint of G, and G^{ij} denotes the complement minor corresponding to g_{ij}.

According to the post-multiplication between a square matrix and a diagonal matrix, the controllers of each column in C_s can be derived from eq 3 as follows:

$$c_{ji} = \frac{G^{ij}}{\det(G)}h_{r,i} \qquad (\text{for } i,j = 1, 2, ..., m) \tag{4}$$

Let

$$p_{ij} = \frac{G^{ij}}{\det(G)} = p_{0,ij}e^{L_{ij}s} \qquad (\text{for } i,j = 1, 2, ..., m) \tag{5}$$

where $p_{0,ij}$ denotes the "delay-free" portion of p_{ij}; that is, at least one term in either of the numerator or denominator polynomials of $p_{0,ij}$ does not include any time delay. We then define the "inverse relative degree" of $p_{0,ij}$ to be n_{ij}, i.e., the largest integer that satisfies

$$\lim_{s\to\infty}\frac{s^{n_{ij}-1}}{p_{0,ij}}=0 \tag{6}$$

and let

$$\theta_{r,i}=\max\{L_{ij};\, j=1, 2, ..., m\} \qquad (\text{for } i=1, 2, ..., m) \tag{7}$$

$$n_{r,i}=\max\{n_{ij};\, j=1, 2, ..., m\} \qquad (\text{for } i=1, 2, ..., m) \tag{8}$$

Equation 4 shows that each column controller in C_s are associated with the same diagonal element in H_r; i.e., all of c_{ji} ($j = 1, 2, ..., m$) correspond to the same $h_{r,i}$ for $i = 1, 2, ..., m$. Note that $\theta_{r,i}$ ($i = 1, 2, ..., m$) defined in eq 7 is positive, which can be identified through eq 5 using the algebra of a linear matrix. Some or even all of the ith column controllers c_{ji} ($j = 1, 2, ..., m$) derived in eq 4 may not be realizable if the corresponding diagonal element $h_{r,i}$ in H_r does not include an equivalent time delay to offset $\theta_{r,i}$. This constraint is due to the fact that each output can respond to the corresponding set-point change only after certain time delay arising from the process characteristics. Equation 4 also shows that, if the relative degree of the delay-free portion of $h_{r,i}$ were less than $n_{r,i}$, some or even all of c_{ji} ($j = 1, 2, ..., m$) would not be proper and thus cannot be implemented physically. Besides, det(G) may include RHP zeros that are not canceled out by the common RHP zeros of G^{ij} ($j = 1, 2, ..., m$). If $h_{r,i}$ does not include these RHP zeros, each of c_{ji} ($j = 1, 2, \cdots, m$) would be bundled with unstable poles, which is definitely not allowed in practice.

Combining the aforementioned practical constraints with the H_2 optimal performance objective,[14] the desired diagonal elements in H_r are proposed in the form of

$$h_{r,i}=\frac{e^{-\theta_{r,i}s}}{(\lambda_{c,i}s+1)^{n_{r,i}}}\prod_{k=1}^{q_i}\frac{-s+z_k}{s+z_k^*} \quad (\text{for } i=1, 2, ..., m) \tag{9}$$

where $\lambda_{c,i}$ is an adjustable parameter set for tuning the desired tracking performance for the ith process output, z_k ($k = 1, 2, ..., q_i$) are the RHP zeros of det(G), excluding those canceled out by the common RHP zeros of G^{ij} ($j = 1, 2, ..., m$), q_i is the total number of such zeros, and z_k^* is the complex conjugate of z_k.

With the desired diagonal elements prescribed in eq 9, it can be ascertained through eqs 4−8 that at least one of each column controller in C_s can be implemented in a proper and rational form, while others of the corresponding column controllers in C_s can be implemented in series with some specified dead-time compensators. Thereby, decoupling regulation for set-point tracking can be realized for individual process outputs.

Note that the closed-loop structure between the process inputs and outputs is used for load-disturbance rejection. The transfer matrix of load-disturbance response (from LD to Y, shown in Figure 1) can be derived as

$$H_d=G(I+C_fG)^{-1} \tag{10}$$

Correspondingly, the closed-loop complementary sensitivity function matrix can be obtained as

$$T_d=C_fG(I+C_fG)^{-1} \tag{11}$$

Notice that it is actually equivalent to the transfer matrix from the load-disturbance vector, LD $= [d_i]_{m\times 1}$, to the controller matrix output vector, $F = [f_i]_{m\times 1}$.

Ideally, it is expected that, when a load disturbance d_i seeps into the ith process input, the resulting system output error, $E = [e_i]_{m\times 1}$, should be detected by the controller matrix C_f immediately after the process time delay, and then C_f yields a control output signal f_i (i.e., $F = [0, 0, ..., f_i, 0, ...,0]^T_{1\times m}$) to act against this disturbance. To counterbalance multiple load disturbances that respectively seep into the process inputs at different times, $\mathbf{T}_d$ is desired to be a diagonal transfer matrix, i.e., $\mathbf{T}_d = \mathrm{diag}[t_{d,i}]_{m\times m}$, so that the control output signals f_i ($i = 1, 2, ..., m$) can be separately tuned for optimization. In this way, each of the load-disturbance responses can be independently regulated in a transparent manner.

Given that observation, the inverse of $\mathbf{T}_d$, i.e., $\mathbf{T}_d^{-1}$, is also a diagonal matrix if $\mathbf{T}_d$ itself is obtained as a diagonal transfer matrix; we can derive, from eq 11, that

$$C_f=(\mathbf{T}_d^{-1}-I)^{-1}G^{-1} \tag{12}$$

Correspondingly, each row controller in C_f can be obtained as

$$cf_{ij}=\frac{t_{d,i}}{1-t_{d,i}}\times\frac{G^{ji}}{\det(G)} \qquad (\text{for } i,j=1, 2, ..., m) \tag{13}$$

Equation 13 shows that each row controller in C_f are associated with the same diagonal element in $\mathbf{T}_d$; that is, all of cf_{ij} ($j = 1, 2, ..., m$) correspond to the same $t_{d,i}$ for $i = 1, 2, ..., m$.

Using the definitions given in eqs 5 and 6, we let

$$\theta_{d,i}=\max\{L_{ji};\, j=1, 2, ..., m\} \qquad (\text{for } i=1, 2, ..., m) \tag{14}$$

$$n_{d,i}=\max\{n_{ji};\, j=1, 2, ..., m\} \qquad (\text{for } i=1, 2, ..., m) \tag{15}$$

Thus, we can follow the analysis on implementation constraints for eq 4 to determine the practical desired forms of $t_{d,i}$ ($i = 1, 2, ..., m$), based on the H_2 optimal performance objective.

In fact, there are four possible cases of the RHP zero distribution of det(G) as categorized in the work by Liu et al.:[24]

(1) No RHP zero;

(2) Finite RHP zeros, for which z_k ($k = 1, 2, ..., q_i$) are the RHP zeros of det(G), excluding those canceled out by the common RHP zeros of G^{ij} (or G^{ji}) ($j = 1, 2, ..., m$);

(3) Infinite RHP and left-half-plane (LHP) zeros, for which z_k ($k = 1, 2, ..., q_i$) are the dominant RHP zeros of det(G), excluding those canceled out by the common RHP zeros of G^{ij} (or G^{ji}) ($j = 1, 2, ..., m$); and

(4) Infinite RHP but finite LHP zeros, for which z_k ($k = 1, 2, ..., q_i$) are the LHP zeros of det(G) excluding those equal to the complex conjugates of the common RHP zeros of G^{ij} (or G^{ji}) ($j = 1, 2, ..., m$), and det(G) may be reformulated as

$$\det(G)=\frac{\phi(s)e^{-\theta_{\min}s}}{\psi(s)}$$

where $\psi(s)$ is the least common denominator of all terms of deg(G), $\phi(s)$ is the corresponding numerator polynomial, in which there exists at least one rational term that does not include any time delay, and $\theta_{\min}$ (or $\theta_{\max}$) is the minimum (or the maximum) of time delay factors in deg(G).

For clarity, the desired forms of H_r and T_d are summarized in Table 1, according to the aforementioned categorization of the RHP zero distribution of det(G). Note that the RHP zero number of det(G) can be ascertained by observing its Nyquist curve. Equation 1 shows that det(G) has no RHP pole. Thus,

Table 1. Summarization of Desired Transfer Matrices and Controller Matrices

case	$h_{r,i}$ $(i = 1, 2, ..., m)$	$t_{d,i}$ $(i = 1, 2, ..., m)$	c_{ji} $(i,j = 1, 2, ..., m)$	$cf_{ij}(i, j = 1, 2, ..., m)$
1	$h_{r,i}^1 = \dfrac{e^{-\theta_{r,i}s}}{(\lambda_{c,i}s + 1)^{n_{r,i}}}$	$t_{d,i}^1 = \dfrac{e^{-\theta_{d,i}s}}{(\lambda_{f,i}s + 1)^{n_{d,i}}}$	$\dfrac{D_{ij}e^{-(\theta_{r,i}-L_{ij})s}}{(\lambda_{c,i}s + 1)^{n_{r,i}}}, \quad D_{ij} = p_{0,ij}$	$\dfrac{D_{ij}e^{-(\theta_{d,i}-L_{ji})s}}{(\lambda_{f,i}s + 1)^{n_{d,i}}} \times \dfrac{1}{1 - \left[\dfrac{e^{-\theta_{d,i}s}}{(\lambda_{f,i}s + 1)^{n_{d,i}}}\right]}, \quad D_{ji} = p_{0,ji}$
2 or 3	$h_{r,i}^1 \prod_{k=1}^{q_i} \dfrac{-s + z_k}{s + z_k^*}$	$t_{d,i}^1 \prod_{k=1}^{q_i} \dfrac{-s + z_k}{s + z_k^*}$	$\dfrac{D_{ij}e^{-(\theta_{r,i}-L_{ij})s}}{(\lambda_{c,i}s + 1)^{n_{r,i}} \prod_{k=1}^{q_i}(s + z_k^*)}$ $D_{ij} = p_{0,ij} \prod_{k=1}^{q_i}(-s + z_k)$	$\dfrac{D_{ji}e^{-(\theta_{d,i}-L_{ji})s}}{(\lambda_{f,i}s + 1)^{n_{d,i}} \prod_{k=1}^{q_i}(s + z_k^*)} \times \dfrac{1}{1 - \dfrac{e^{-\theta_{d,i}s}}{(\lambda_{f,i}s + 1)^{n_{d,i}}} \prod_{k=1}^{q_i}\dfrac{-s + z_k}{s + z_k^*}}$ $D_{ji} = p_{0,ji} \prod_{k=1}^{q_i}(-s + z_k)$
4	$\dfrac{h_{r,i}^1 \phi(s) e^{(\theta_{max}-\theta_{min})s}}{\phi(-s)} \prod_{k=1}^{q_i} \dfrac{-s - z_k}{s - z_k^*}$	$\dfrac{t_{d,i}^1 \phi(s) e^{(\theta_{max}-\theta_{min})s}}{\phi(-s)} \prod_{k=1}^{q_i} \dfrac{-s - z_k}{s - z_k^*}$	$\dfrac{G^{ji}D_{ji}\psi(s)e^{(\theta_{min}-\theta_{r,i})s}}{(\lambda_{c,i}s + 1)^{n_{r,i}} \prod_{k=1}^{q_i}(s - z_k^*)}$, $D_{ij} = \dfrac{e^{(\theta_{max}-\theta_{min})s}}{\phi(-s)} \prod_{k=1}^{q_i}(s - z_k)$	$\dfrac{G_{ij}D_{ij}\psi(s)e^{(\theta_{min}-\theta_{d,i})s}}{(\lambda_{f,i}s + 1)^{n_{d,i}} \prod_{k=1}^{q_i}(s - z_k^*)} \times \dfrac{1}{1 - \dfrac{D_{ji}\phi(s)e^{-\theta_{d,i}s}}{(\lambda_{f,i}s + 1)^{n_{d,i}} \prod_{k=1}^{q_i}(-s - z_k^*)}}$, $D_{ji} = \dfrac{e^{(\theta_{max}-\theta_{min})s}}{\phi(-s)} \prod_{k=1}^{q_i}(-s - z_k)$

the number of its Nyquist curve encircling the origin is exactly equal to its RHP zero number, according to the Nyquist stability criterion. Alternatively, the RHP zeros of det(G) can be derived explicitly using any numerical solution method or mathematical software package.

4. Controller Matrix Design

With the desired H_r and T_d values, as listed in Table 1, the ideally desired set-point tracking controller matrix C_s and the closed-loop controller matrix C_f for load-disturbance rejection can be derived from eqs 4 and 13, respectively. For instance, with case 2, that det(G) has finite RHP zeros, the controllers of each column in C_s and the controllers of each row in C_f can be respectively derived as

$$c_{ji} = \frac{D_{ij} e^{-(\theta_{r,i}-L_{ij})s}}{(\lambda_{c,i}s+1)^{n_{r,i}} \prod_{k=1}^{q_i}(s+z_k^*)} \qquad (\text{for } i, j = 1, 2, ..., m) \tag{16}$$

$$cf_{ij} = \frac{D_{ji} e^{-(\theta_{d,i}-L_{ji})s}}{(\lambda_{f,i}s+1)^{n_{d,i}} \prod_{k=1}^{q_i}(s+z_k^*)} \times \frac{1}{1-\dfrac{e^{-\theta_{d,i}s}}{(\lambda_{f,i}s+1)^{n_{d,i}}} \prod_{k=1}^{q_i}\dfrac{-s+z_k}{s+z_k^*}} \qquad (\text{for } i, j = 1, 2, ..., m) \tag{17}$$

where $\lambda_{c,i}$ is the common adjustable parameter of the controllers of each column in C_s and $\lambda_{f,i}$ is the common adjustable parameter of the controllers of each row in C_f, and

$$D_{ij} = p_{0,ij} \prod_{k=1}^{q_i}(-s+z_k) \tag{18}$$

$$D_{ji} = p_{0,ji} \prod_{k=1}^{q_i}(-s+z_k) \tag{19}$$

Equation 5 indicates that both D_{ij} and D_{ji} are not of a rational transfer function for a MIMO process with time delays and, thus, are difficult to be implemented in practice. Besides, the RHP zeros of det(G) will result in RHP zero-pole cancellation in D_{ij} and D_{ji}, causing C_s and C_f to behave in an unstable manner. Therefore, the analytical approximation method developed by Liu et al.[24] is adopted to copy the rational and stable forms of D_{ij} and D_{ji} for implementation, by

$$D_{U/V} = \frac{\sum_{k=0}^{U} a_k s^k}{\sum_{k=0}^{V} b_k s^k} \tag{20}$$

where U and V are the user-specified orders to achieve the desirable system performance specification, and the constant coefficients a_k ($k = 1, 2, ..., U$) and b_k ($k = 1, 2, ..., V$) are determined by the following two matrix equations:

$$\begin{bmatrix} a_0 \\ a_1 \\ \vdots \\ a_U \end{bmatrix} = \begin{bmatrix} d_0 & 0 & 0 & \cdots & 0 \\ d_1 & d_0 & 0 & \cdots & 0 \\ \vdots & \vdots & \ddots & \cdots & \vdots \\ d_U & d_{U-1} & d_{U-2} & \cdots & d_{U-V} \end{bmatrix} \begin{bmatrix} b_0 \\ b_1 \\ \vdots \\ b_V \end{bmatrix} \tag{21}$$

$$\begin{bmatrix} d_U & d_{U-1} & \cdots & d_{U-V+1} \\ d_{U+1} & d_U & \cdots & d_{U-V+2} \\ \vdots & \vdots & \ddots & \vdots \\ d_{U+V-1} & d_{U+V-2} & \cdots & d_U \end{bmatrix} \begin{bmatrix} b_1 \\ b_2 \\ \vdots \\ b_V \end{bmatrix} = -\begin{bmatrix} d_{U+1} \\ d_{U+2} \\ \vdots \\ d_{U+V} \end{bmatrix} \tag{22}$$

where d_k ($k = 0, 1, ..., U + V$) are the constant coefficients of each term in the Maclaurin series of D_{ij} (or D_{ji}), i.e.,

$$d_k = \frac{1}{k!} \lim_{s\to 0} \frac{d^k D_{ij}}{ds^k} \qquad (\text{for } k = 0, 1, ..., U+V) \tag{23}$$

and b_0 should be chosen as

$$b_0 = \begin{cases} 1 & (\text{for } b_k \geq 0) \\ -1 & (\text{for } b_k < 0) \end{cases} \tag{24}$$

Note that the second portion of cf_{ij} shown in eq 17 has the following properties:

$$\lim_{s\to\infty} \frac{1}{1-\dfrac{e^{-\theta_{d,i}s}}{(\lambda_{f,i}s+1)^{n_{d,i}}} \prod_{k=1}^{q_i}\dfrac{-s+z_k}{s+z_k^*}} = 1 \tag{25}$$

$$\lim_{s\to 0} \frac{1}{1-\dfrac{e^{-\theta_{d,i}s}}{(\lambda_{f,i}s+1)^{n_{d,i}}} \prod_{k=1}^{q_i}\dfrac{-s+z_k}{s+z_k^*}} = \infty \tag{26}$$

Thus, it can be regarded as a special integrator with zero relative degree for eliminating the system output error. This integrator can be practically implemented using a positive feedback control unit, as suggested in the work by Liu et al.[24]

For the other cases of the RHP zero distribution of det(G), as categorized in section 3, the corresponding executable forms of C_s and C_f can be derived analytically, following a procedure similar to that previously described. The results are summarized in Table 1.

Remark 2. D_{ij} (or D_{ji}) of all the cases in Table 1 can be approximated in a rational form for implementation using eqs 20−24. For the first three cases of Table 1, D_{ij} (or D_{ji}) can also be factorized as two portions, as $D_{ij} = G^{ij}D_{0,ij}$ (or $D_{ji} = G^{ji}D_{0,ji}$), such that only the second portion $D_{0,ij}$ (or $D_{0,ji}$) must be transformed for implementation. Such an exercise may relieve the computation effort or can be explored to obtain a better approximation, but at the cost of higher implementation complexity. For the convenience of implementation, low-order approximation such as 2 or 3 is primarily recommended in practice.

◇

5. System Stability Analysis

Because the ideally desired set-point tracking controller matrix and closed-loop controller matrix are approximated analytically for practical implementation, the stability of the resulting control system should be checked. Besides, there usually exist the

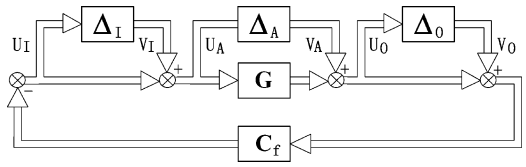

Figure 2. Closed-loop structure with the process additive, multiplicative input, and output uncertainties.

unmodeled process dynamics in practice. Assessment of the control system robust stability should be conducted in the presence of process uncertainties, together with an on-line tuning rule of the adjustable parameters of the two controller matrices to accommodate the process uncertainties.

In the nominal case of no process uncertainty, Figure 1 shows that evaluation of the control system stability can be limited to the closed-loop structure set between the process inputs and outputs, provided that the set-point tracking controller matrix C_s is configured to be stable. As far as the closed-loop structure is concerned, the inputs are *U*, *LD*, Y_r, and *N*, and the outputs are *Y* and *F*. Note that *U* and *LD* have similar impact on the closed-loop structure and so do Y_r and *N*. Hence, evaluation of the nominal system stability can be further limited to the transfer matrix from *LD* and *N* to *Y* and *F*, i.e.,

$$\begin{bmatrix} Y \\ F \end{bmatrix} = \begin{bmatrix} G(I + C_f G)^{-1} & -GC_f(I + GC_f)^{-1} \\ C_f G(I + C_f G)^{-1} & C_f(I + GC_f)^{-1} \end{bmatrix} \begin{bmatrix} LD \\ N \end{bmatrix} \quad (27)$$

Apparently, if all of the elements in the transfer matrix shown in eq 27 are conducted stable, the closed-loop internal stability can be guaranteed such that the entire control system stability can be ensured. To relieve the computation effort for checking the stability of the aforementioned transfer matrix, a simplified stability condition is given in the following Corollary 1, based on the stability theorems developed for a conventional unity feedback control structure.[16]

Corollary 1. The nominal control system holds internal stability if and only if $(I + C_f G)^{-1}$ is kept stable.

Proof. It can be verified, using the following equivalent relationships:

$$C_f G(I + C_f G)^{-1} = I - (I + C_f G)^{-1} \quad (28)$$

$$C_f G(I + C_f G)^{-1} = C_f(I + GC_f)^{-1} G \quad (29)$$

□

Remark 3. The stability of $(I + C_f G)^{-1}$ can be assessed by checking to determine if $\det(I + C_f G)$ has any RHP zeros, which can be performed using the Nyquist curve criterion or any numerical solution method.

◇

In the presence of the process uncertainties, the robust stability analysis can also be limited to the closed-loop structure, because of the open-loop control nature for set-point tracking. The process additive (Δ_A), multiplicative input (Δ_I), and output uncertainties (Δ_O), as shown in Figure 2, are most commonly encountered in practice. In fact, other types of process unstructured or structured uncertainties may be considered to be the combination of the aforementioned process uncertainties to be addressed in practice.[15] Therefore, the following robust stability analysis based on the aforementioned process uncertainties, without loss of generality, can be utilized to evaluate the control system robust stability in the presence of a wide variety of process uncertainties.

By reorganizing the perturbed closed-loop structure shown in Figure 2 in the form of the standard $M-\Delta$ structure for robustness analysis,[16] we can derive the transfer matrices from the outputs to the inputs of Δ_I, Δ_A, and Δ_O,

$$\begin{bmatrix} U_I \\ U_A \\ U_O \end{bmatrix} = M \begin{bmatrix} V_I \\ V_A \\ V_O \end{bmatrix} \quad (30)$$

where

$$M = \begin{bmatrix} -(I + C_f G)^{-1} C_f G & -(I + C_f G)^{-1} C_f & -(I + C_f G)^{-1} C_f \\ (I + C_f G)^{-1} & -(I + C_f G)^{-1} C_f & -(I + C_f G)^{-1} C_f \\ (I + GC_f)^{-1} G & (I + GC_f)^{-1} & -(I + GC_f)^{-1} GC_f \end{bmatrix} \quad (31)$$

Note that there exist equivalent transformations, as shown below:

$$(I + C_f G)^{-1} C_f G = I - (I + C_f G)^{-1} \quad (32)$$

$$(I + GC_f)^{-1} = I - (I + GC_f)^{-1} GC_f \quad (33)$$

Using the equivalent transformation

$$C_f(I + GC_f) = (I + C_f G) C_f \quad (34)$$

yields

$$(I + C_f G)^{-1} C_f = C_f(I + GC_f)^{-1} \quad (35)$$

Besides, it follows from eq 29 that

$$(I + GC_f)^{-1} GC_f = G(I + C_f G)^{-1} C_f \quad (36)$$

Hence, it can be concluded from eqs 28, 29, and 32−36 that *M* holds stability if the nominal control system is constructed in a stable manner, i.e., $(I + C_f G)^{-1}$ is kept stable.

We then can use the multivariable spectral radius stability criterion[15] to obtain the robust stability constraint, i.e.,

$$\rho(M\Delta) < 1, \quad \forall\, \omega \in [0, \infty) \quad (37)$$

For instance, in the presence of the process additive uncertainties, the spectral radius stability constraint can be derived as

$$\rho((I + C_f G)^{-1} C_f \Delta_A) < 1, \quad \forall\, \omega \in [0, \infty) \quad (38)$$

When evaluating the control system robust stability with the process multiplicative input and output uncertainties, the spectral radius stability constraint can be derived as

$$\rho\left(\begin{bmatrix} -(I + C_f G)^{-1} C_f G & -(I + C_f G)^{-1} C_f \\ (I + GC_f)^{-1} G & -(I + GC_f)^{-1} GC_f \end{bmatrix} \begin{bmatrix} \Delta_I & 0 \\ 0 & \Delta_O \end{bmatrix}\right) < 1, \quad \forall\, \omega \in [0, \infty) \quad (39)$$

In fact, the spectral radius stability constraints shown in eqs 38 and 39 can be checked graphically by observing whether the magnitude plots of spectral radius fall below the unity for $\omega \in [0, +\infty)$. Such exercise can be performed using any commercial control software packages (e.g., MATLAB control toolbox). In this way, the admissible tuning range of the

adjustable parameters of C_f can be ascertained. For a specified bound of Δ_A, Δ_I, or Δ_O, in practice, eqs 38 and 39 may be used to evaluate the control system robust stability, as illustrated in example 2 of section 6.

Combining the desired transfer matrices shown in Table 1 with eqs 2 and 11, we can see that when the adjustable parameter $\lambda_{c,i}$ ($i = 1, 2, ..., m$) in C_s is tuned to a smaller value, the corresponding ith system output response for set-point tracking becomes faster, but the output commands of the ith column controllers in C_s and the corresponding actuators will be required larger, tending to exceed their output capacities in practice. Accordingly, more aggressive dynamic behavior of the ith system output response will be yielded in the presence of process uncertainties. In contrast, gradually increasing $\lambda_{c,i}$ will slow the corresponding ith system output response, whereas the output commands of the ith column controllers in C_s and the corresponding actuators can be reduced. Consequently, less aggressive dynamic behavior of the ith system output response will appear in the presence of process uncertainties. Thereby, on-line tuning of $\lambda_{c,i}$ ($i = 1, 2, ..., m$) aims at the tradeoff between the achievable set-point tracking performance and the output capacities of C_s and its corresponding actuators. In a similar manner, decreasing the adjustable parameter $\lambda_{f,i}$ ($i = 1, 2, ..., m$) in C_f may enhance the closed-loop performance for rejecting the load disturbance d_i that seeps into the ith process input, but the output commands of the ith row controllers in C_f and the corresponding actuators will be required larger, leading to degraded robust stability of the closed-loop structure, and vice versa. Therefore, on-line tuning of $\lambda_{f,i}$ ($i = 1, 2, ..., m$) in C_f aims at the tradeoff between the nominal closed-loop performance for load-disturbance rejection and its robust stability in the presence of process uncertainties. Based on a large quantity of simulation studies, it is recommended to initially set $\lambda_{c,i}$ and $\lambda_{f,i}$ respectively in the range of $1.0(\theta_{r,i})-(10\theta_{r,i})$ and $1.0(\theta_{d,i})-10(\theta_{d,i})$ for $i = 1, 2, ..., m$, and then adjust them monotonously online to achieve a desirable performance specification for set-point tracking and load-disturbance rejection.

6. Illustration

Two benchmark examples are adopted here to demonstrate the effectiveness and merits of the proposed 2-DOF decoupling control scheme. The first example involves the case where the process transfer matrix determinant has no RHP zero, whereas the second example is for an opposite case.

Example 1. Consider the 3×3 process that has been widely studied in the literature (see, e.g., refs 23, 24, and 38):

$$G = \begin{bmatrix} \dfrac{1.986e^{-0.71s}}{66.7s+1} & \dfrac{-5.24e^{-60s}}{400s+1} & \dfrac{-5.984e^{-2.24s}}{14.29s+1} \\ \dfrac{-0.0204e^{-0.59s}}{(7.14s+1)^2} & \dfrac{0.33e^{-0.68s}}{(2.38s+1)^2} & \dfrac{-2.38e^{-0.42s}}{(1.43s+1)^2} \\ \dfrac{-0.374e^{-7.75s}}{22.22s+1} & \dfrac{11.3e^{-3.79s}}{(21.74s+1)^2} & \dfrac{9.811e^{-1.59s}}{11.36s+1} \end{bmatrix}$$

It can be verified, using the Nyquist curve criterion, that there is no RHP zero in det(G) and, thus, it belongs to case 1 in Table 1. The use of eq 5 yields $L_{11} = 0.71$, $L_{12} = 0.8$, and $L_{13} = -1.4$. A value of $\theta_{r,1} = 0.8$ thereby can be obtained from eq 7. Using eq 6 then yields values of $n_{11} = 1$, $n_{12} = 1$, and $n_{13} = 0$;therefore, a value of $n_{r,1} = 1$ can be obtained from eq 8. Similarly, the use of eqs 5−8 yields values of $\theta_{r,2} = 0.68$, $\theta_{r,2} = 1.85$, and $n_{r,2} = 2$, $n_{r,3} = 1$. According to the design formula for case 1 in Table 1, the diagonal elements in the desired system response transfer matrix can be determined as

$$h_{r,1} = \frac{e^{-0.8s}}{\lambda_{c,1}s+1}$$

$$h_{r,2} = \frac{e^{-0.68s}}{(\lambda_{c,2}s+1)^2}$$

$$h_{r,3} = \frac{e^{-1.85s}}{\lambda_{c,3}s+1}$$

Correspondingly, the set-point tracking controller matrix can be derived using the design formula for case 1 in Table 1. To obtain the same controller orders as those of the recent decoupling control method[24] for fair comparison, which are similar to those from Huang et al.[38] (full form) and Wang et al.,[23] the controller matrix form for set-point tracking is given in the Appendix.

The use of eqs 14 and 15 yields $\theta_{d,1} = 0.71$, $\theta_{d,2} = 1.85$, and $\theta_{d,3} = 1.59$, and $n_{d,1} = n_{d,3} = 1$, and $n_{d,2} = 2$. Thus, the closed-loop controller matrix can also be derived using the design formula for case 1, which is also listed in the Appendix with controller orders that are similar to those for set-point tracking.

To obtain a rising speed for set-point tracking similar to that of Huang et al.[38] and Wang et al.,[23] the adjustable parameters in C_s are taken as $\lambda_{c,1} = 8$, $\lambda_{c,2} = 10$, and $\lambda_{c,3} = 15$, and the adjustable parameters in C_f are taken as $\lambda_{f,1} = 0.2$, $\lambda_{f,2} = 18$, and $\lambda_{f,3} = 15$, to compare with Huang et al.[38] for load-disturbance rejection. By adding a unit step change at the moments of $t = 0$, 300, and 600 s, respectively, to the ternary set-point inputs, and an inverse step change of load disturbances to the ternary process outputs at $t = 900$ s with a dynamic of

$$G_L = \left[\frac{1.986e^{-0.71s}}{66.7s+1}, \frac{-0.0204e^{-3.53s}}{11.49s+1}, \frac{-0.374e^{-7.75s}}{22.22s+1}\right]^T$$

as used in Huang and Lin,[38] the resulting system output responses are shown in Figure 3.

Figure 3 clearly shows that the ternary set-point responses without overshoot have been obtained using the proposed scheme (solid line), and the ternary process output responses are almost entirely decoupled from each other. Moreover, both the proposed scheme and Huang et al.[38] have led to obviously enhanced load-disturbance rejection, because of the use of 2-DOF control structure. The same set-point tracking performance is obtained using the proposed 2-DOF control scheme and the decoupling scheme based on a unity feedback control structure,[24] because of the use of the same controller orders and adjustable parameters for set-point tracking. Note that better system performance for both set-point tracking and load-disturbance rejection can be conveniently obtained in the proposed 2-DOF control scheme by monotonously decreasing the adjustable parameters of C_s and C_f online.

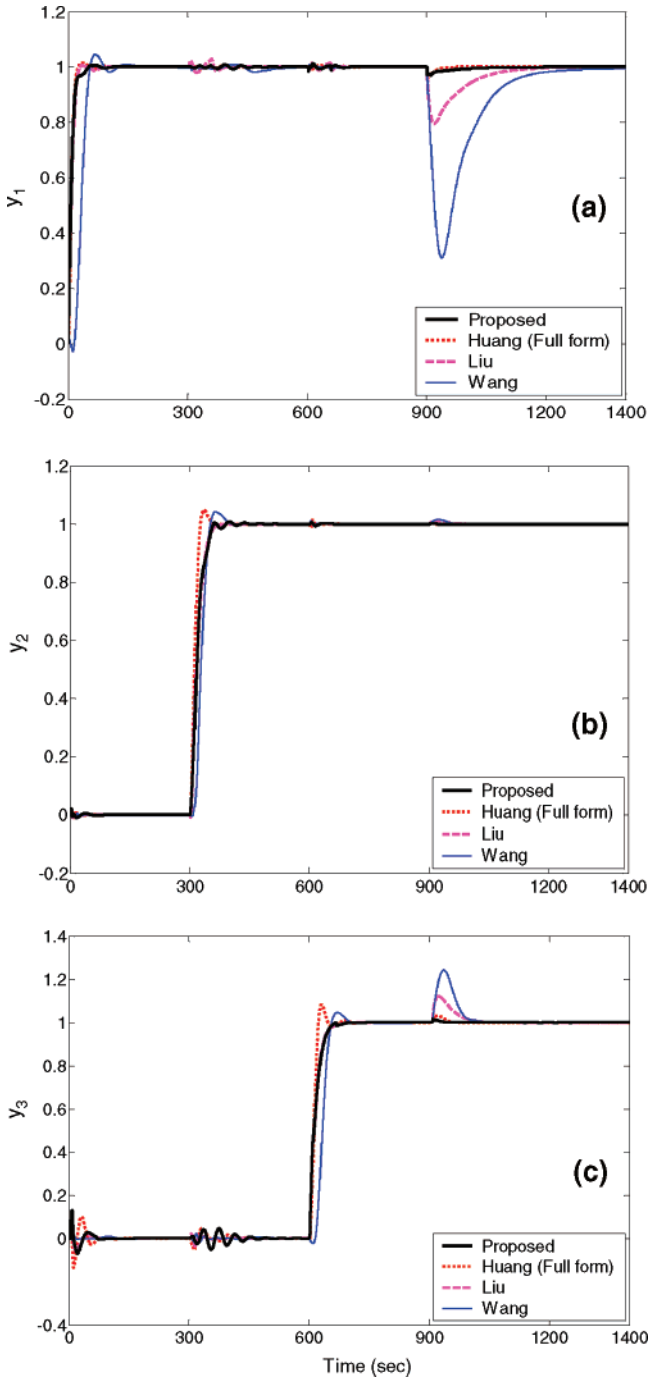

Figure 3. Nominal system output responses for example 1: (a) y_1, (b) y_2, and (c) y_3.

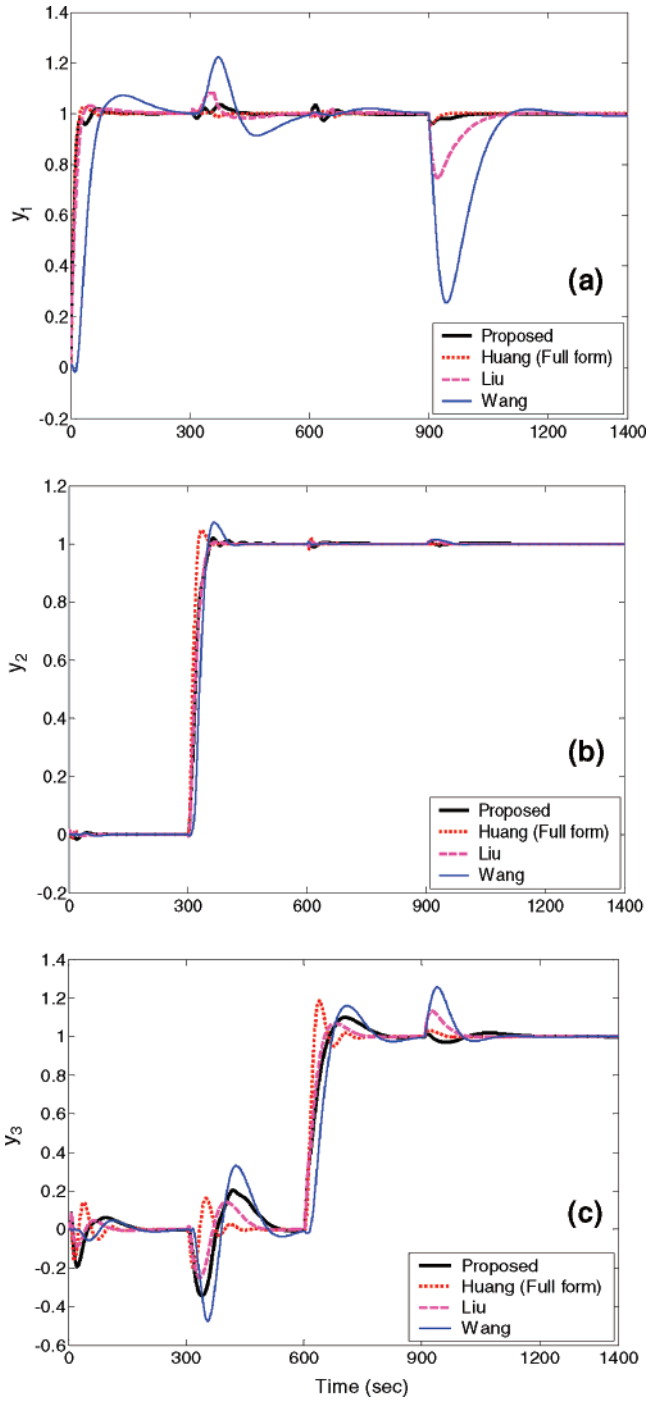

Figure 4. Perturbed system output responses for example 1: (a) y_1, (b) y_2, and (c) y_3.

To demonstrate the robust stability of the proposed 2-DOF control scheme, one of the process parameter perturbation tests in Wang's method[23] is performed here; that is, all the time constants of each element in the process transfer matrix are assumed to be actually 40% larger, to introduce the unmodeled process dynamics. The perturbed system output responses are shown in Figure 4, indicating that the proposed control system(solid line) holds robust stability well in the presence of the severe process parameters perturbation. Note that better robust stability can be conveniently obtained in the proposed control system by monotonously increasing the adjustable parameters of C_f online.

Example 2. Consider the binary process studied in the literature (see, e.g., refs 21, 38, and 39):

$$G = \begin{bmatrix} \dfrac{(-s+1)e^{-2s}}{s^2+1.5s+1} & \dfrac{0.5(-s+1)e^{-4s}}{(2s+1)(3s+1)} \\ \dfrac{0.33(-s+1)e^{-6s}}{(4s+1)(5s+1)} & \dfrac{(-s+1)e^{-3s}}{4s^2+6s+1} \end{bmatrix}$$

Obviously, there is a common RHP zero ($s = 1$) of each element in the process transfer matrix. Thus, it is a dual RHP zero of det(G). It can be verified that det(G) has no other RHP zeros. Using eqs 5−8 yields values of $\theta_{r,1} = 2$, $\theta_{r,2} = 3$, and $n_{r,1} = n_{r,2} = 1$. According to the design formula for case 2 in Table 1,

the set-point tracking controller matrix can be derived as

$$C_s = D\cdot\begin{bmatrix} \dfrac{s^2+1.5s+1}{(\lambda_{c,1}s+1)(s+1)} & -\dfrac{0.5(s^2+1.5s+1)(4s^2+6s+1)e^{-2s}}{(\lambda_{c,2}s+1)(s+1)(2s+1)(3s+1)} \\ -\dfrac{0.33(s^2+1.5s+1)(4s^2+6s+1)e^{-3s}}{(\lambda_{c,1}s+1)(s+1)(4s+1)(5s+1)} & \dfrac{4s^2+6s+1}{(\lambda_{c,2}s+1)(s+1)} \end{bmatrix}$$

where

$$D = \frac{1}{1-\dfrac{0.165(s^2+1.5s+1)(4s^2+6s+1)}{(2s+1)(3s+1)(4s+1)(5s+1)}e^{-5s}}$$

Using eqs 14 and 15 yields values of $\theta_{d,1} = 2$, $\theta_{d,2} = 3$, and $n_{d,1} = n_{d,2} = 1$. Therefore, the closed-loop controller matrix can be similarly derived as

$$C_f = D\cdot\begin{bmatrix} \dfrac{s^2+1.5s+1}{(\lambda_{f,1}s+1)(s+1)}D_1 & -\dfrac{0.5(s^2+1.5s+1)(4s^2+6s+1)e^{-s}}{(\lambda_{f,1}s+1)(s+1)(2s+1)(3s+1)}D_1 \\ -\dfrac{0.33(s^2+1.5s+1)(4s^2+6s+1)e^{-4s}}{(\lambda_{f,2}s+1)(s+1)(4s+1)(5s+1)}D_2 & \dfrac{4s^2+6s+1}{(\lambda_{f,2}s+1)(s+1)}D_2 \end{bmatrix}$$

where

$$D_1 = \frac{1}{1-\dfrac{(-s+1)e^{-2s}}{(\lambda_{f,1}s+1)(s+1)}}$$

and

$$D_2 = \frac{1}{1-\dfrac{(-s+1)e^{-3s}}{(\lambda_{f,2}s+1)(s+1)}}$$

To obtain a set-point tracking speed similar to that of Huang et al.,[38] which had already demonstrated its superiority over Wang et al.[21] and Jerome and Ray,[39] the adjustable parameters of C_s are taken as $\lambda_{c,1} = 2$ and $\lambda_{c,2} = 2$. The adjustable parameters of C_f are taken as $\lambda_{f,1} = 0.8$ and $\lambda_{f,2} = 1.5$, to obtain similar nominal load-disturbance rejection performance. By adding a unit step change at $t = 0$ and 100 s, respectively, to the binary set-point inputs, and an inverse step change of load disturbances to the binary process outputs at $t = 200$ s with a dynamic of

$$G_L = \left[\frac{e^{-s}}{25s+1}, \frac{e^{-s}}{25s+1}\right]^T$$

as used in Huang and Lin,[38] we obtain the system output responses shown in Figure 5. It can be observed that the proposed scheme has resulted in entirely decoupled output responses without overshoot for set-point tracking (shown by the thick solid line). To relieve the implementation of D included in C_s and C_f, a first-order transformation is therefore derived to approximate it, using the rational approximation formula given in eq 20, i.e.,

$$D_{1/1} = \frac{8.227s+1.1976}{9.142s+1}$$

The corresponding system output responses are also provided in Figure 5 for comparison, indicating that very small degradation of system performance is thus yielded.

To compare the control system robust stability, the perturbation test adopted in Wang et al.[21] is performed here (i.e., the static gains and time delays of diagonal elements in the process transfer matrix are assumed to be actually increased by 20% and 30%, respectively). According to the robust stability constraint given in eq 38, the magnitude plot of spectral radius for checking the robust stability is drawn in Figure 6. It is observed that the peak value (shown by the dotted line) is evidently smaller than unity, indicating that the proposed control system is capable of good robust stability. The corresponding system output responses are shown in Figure 7. It can be observed that obviously enhanced robust stability is obtained by the proposed scheme, given the similar nominal performance. Besides, it is illustrated that increasing the common adjustable parameter $\lambda_{c,1}$ of the first column controllers in C_s can gradually suppress oscillation of the set-point response for the process output y_1 in the presence of the process uncertainties, such as the case of $\lambda_{c,1} = 5$ (denoted by the thick solid line in Figure 7). On the other hand, increasing the common adjustable parameter $\lambda_{f,1}$ of the first row controllers in C_f will gradually suppress oscillation of the load-disturbance response for y_1, such as

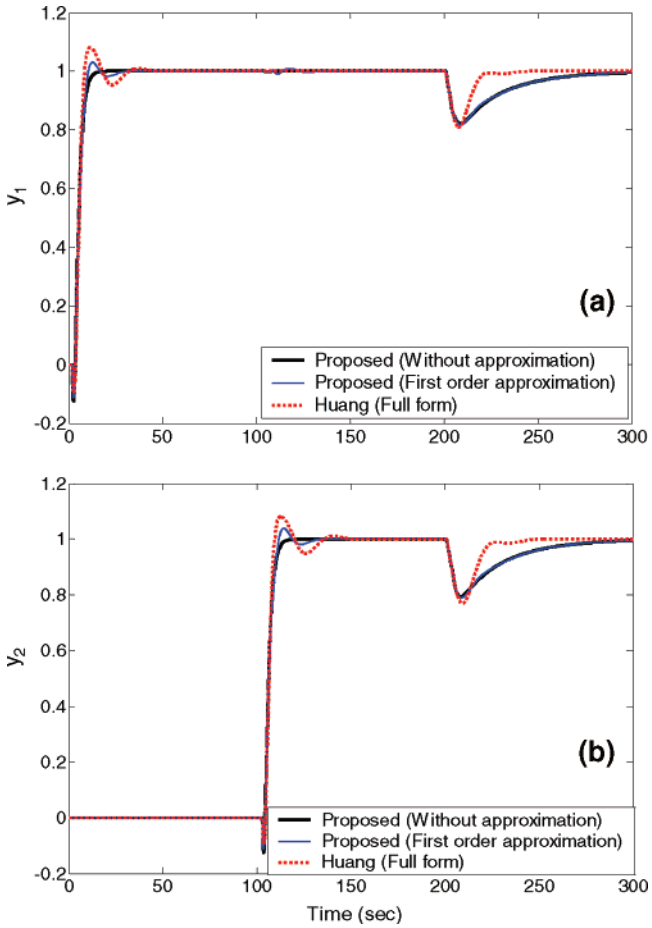

Figure 5. Nominal system output responses for example 2: (a) y_1 and (b) y_2.

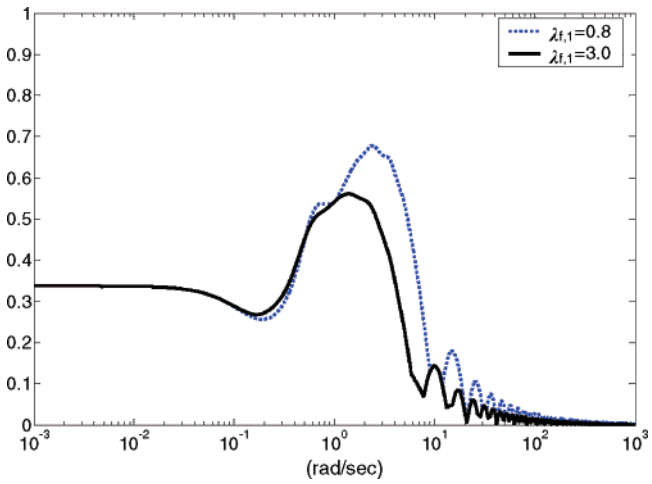

Figure 6. Magnitude plots of spectral radius for example 2.

the case of $\lambda_{f,1} = 3$ shown in Figure 7. Correspondingly, the smaller peak value of spectral radius is yielded as also shown in Figure 6 (solid line), indicating further enhanced system robust stability. Note that both set-point response and load-disturbance response of the process output y_2 are almost not affected by the tuning of $\lambda_{c,1}$ and $\lambda_{f,1}$. It is thus demonstrated that each of the adjustable parameters of C_s can be independently tuned online to optimize the set-point tracking performance of the corresponding process output, and a similar result can be expected for tuning each of the adjustable parameters of C_f to

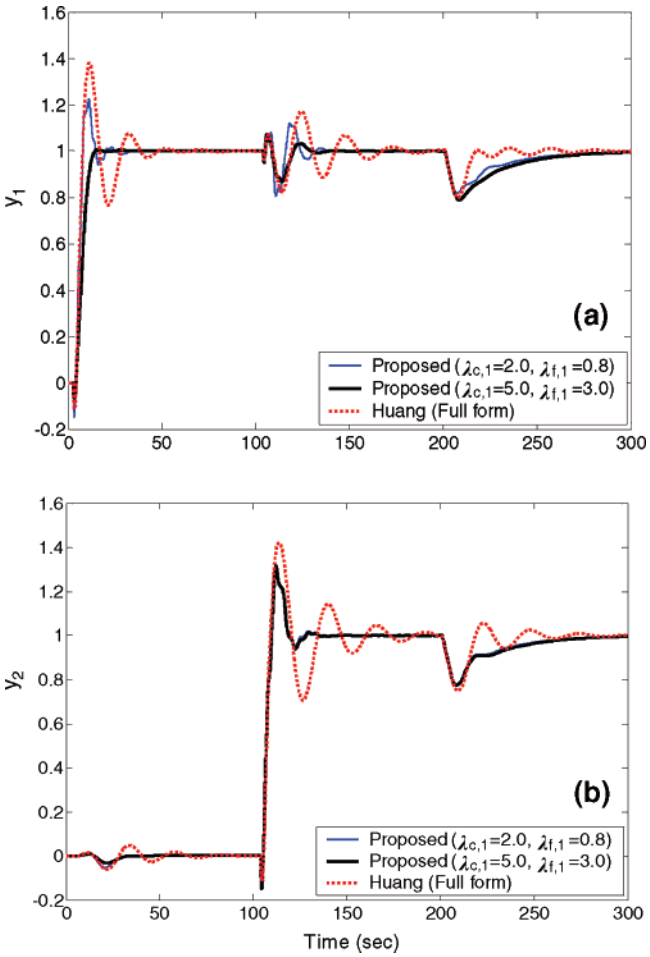

Figure 7. Perturbed system output responses for example 2: (a) y_1 and (b) y_2.

optimize the load-disturbance rejection performance of the corresponding process output.

7. Conclusions

A two-degrees-of-freedom (2-DOF) decoupling control scheme has been proposed for multiple-input−multiple-output (MIMO) processes with time delays. As a result, set-point tracking and load-disturbance rejection can be separately regulated and optimized online, while significant or even absolute decoupling regulation performance can be achieved. The controllers of each column of the set-point tracking controller matrix are tuned in common by a single adjustable parameter, while the controllers of each row in the closed-loop controller matrix for load-disturbance rejection are tuned in common by a different single adjustable parameter. All of these adjustable parameters can be respectively tuned online in a monotonous way to achieve the best tradeoff between the nominal performance of the control system and its robust stability. Moreover, because of the analytical design procedure developed for both the set-point tracking controller matrix and the closed-loop controller matrix, according to the categorization of the RHP zero distribution of det(G) in the complex plane, the computation effort can be significantly relieved in comparison with other recent decoupling control methods based on numerical iteration algorithms. The applications to two benchmark examples have clearly demonstrated the merits of the proposed 2-DOF decoupling control scheme.

Appendix: Controller Matrices for Example 1

$$c_{11} = \frac{14543s^2 + 256.3578s + 0.5502}{(\lambda_{c,1}s + 1)(438.7353s + 1)} e^{-0.09s}$$

$$c_{21} = \frac{12391s^3 + 746.2116s^2 + 9.7508s + 0.0199}{(\lambda_{c,1}s + 1)(3940.3s^2 + 447.8424s + 1)}$$

$$c_{31} = \frac{1736.5s^3 - 21.7287s^2 - 0.8474s - 0.002}{(\lambda_{c,1}s + 1)(4815.4s^2 + 449.8302s + 1)} e^{-2.2s}$$

$$c_{12} = \frac{4773900s^6 - 6620600s^5 - 3286200s^4 - 532380s^3 - 41045s^2 - 526.1791s - 0.296}{(\lambda_{c,2}s + 1)^2(611700s^4 + 109510s^3 + 12128s^2 + 465.9313s + 1)} e^{-3.73s}$$

$$c_{22} = \frac{13471000s^6 + 3306200s^5 + 892990s^4 + 117120s^3 + 6709.9s^2 + 142.0148s + 0.3149}{(\lambda_{c,2}s + 1)^2(336570s^4 + 33465s^3 + 9959.2s^2 + 461.3811s + 1)}$$

$$c_{32} = \frac{-197040s^5 - 104730s^4 - 29099s^3 - 4024.9s^2 - 171.9233s - 0.374}{(\lambda_{c,2}s + 1)^2(257300s^4 + 55907s^3 + 10254s^2 + 461.9346s + 1)} e^{-2.2s}$$

$$c_{13} = \frac{400930s^4 + 33536s^3 + 1342.3s^2 + 31.5279s + 0.2638}{(\lambda_{c,3}s + 1)(33025s^3 + 3869.9s^2 + 447.5041s + 1)} e^{-1.79s}$$

$$c_{23} = \frac{16790s^3 + 1582.9s^2 + 39.2646s + 0.0885}{(\lambda_{c,3}s + 1)(511.4853s^2 + 440.0233s + 1)}$$

$$c_{33} = \frac{2195s^3 + 212.3057s^2 + 5.2157s + 0.01}{(\lambda_{c,3}s + 1)(1319.1s^2 + 441.8636s + 1)} e^{-0.26s}$$

$$cf_{11} = D_1\left[\frac{14543s^2 + 256.3578s + 0.5502}{(\lambda_{f,1}s + 1)(438.7353s + 1)}\right]$$

$$cf_{12} = D_1\left[\frac{-5757900s^5 - 3439700s^4 - 562940s^3 - 41482s^2 - 526.426s - 0.296}{(\lambda_{f,1}s + 1)(615900s^4 + 116360s^3 + 12510s^2 + 466.7655s + 1)}\right] e^{-3.76s}$$

$$cf_{13} = D_1\left[\frac{400930s^4 + 33536s^3 + 1342.3s^2 + 31.5279s + 0.2638}{(\lambda_{f,1}s + 1)(33025s^3 + 3869.9s^2 + 447.5041s + 1)}\right] e^{-0.65s}$$

$$cf_{21} = D_2\left[\frac{12391s^3 + 746.2116s^2 + 9.7508s + 0.0199}{(\lambda_{f,2}s + 1)^2(3940.3s^2 + 447.8424s + 1)}\right] e^{-1.05s}$$

$$cf_{22} = D_2\left[\frac{13471000s^6 + 3306200s^5 + 892990s^4 + 117120s^3 + 6709.9s^2 + 142.0148s + 0.3149}{(\lambda_{f,2}s + 1)^2(336570s^4 + 33465s^3 + 9959.2s^2 + 461.3811s + 1)}\right] e^{-1.17s}$$

$$cf_{23} = D_2\left[\frac{16790s^3 + 1582.9s^2 + 39.2646s + 0.0885}{(\lambda_{f,2}s + 1)^2(511.4853s^2 + 440.0233s + 1)}\right]$$

$$cf_{31} = D_3\left[\frac{1736.5s^3 - 21.7287s^2 - 0.8474s - 0.002}{(\lambda_{f,3}s + 1)(4815.4s^2 + 449.8302s + 1)}\right] e^{-2.99s}$$

$$cf_{32} = D_3\left[\frac{-197040s^5 - 104730s^4 - 29099s^3 - 4024.9s^2 - 171.9233s - 0.374}{(\lambda_{f,3}s + 1)(257300s^4 + 55907s^3 + 10254s^2 + 461.9346s + 1)}\right] e^{-3.11s}$$

$$cf_{33} = D_3\left[\frac{2195s^3 + 212.3057s^2 + 5.2157s + 0.01}{(\lambda_{f,3}s + 1)(1319.1s^2 + 441.8636s + 1)}\right]$$

$$D_1 = \frac{1}{1 - \left(\frac{e^{-0.71s}}{\lambda_{f,1}s + 1}\right)}$$

$$D_2 = \frac{1}{1 - \left(\frac{e^{-1.85s}}{(\lambda_{f,2}s + 1)^2}\right)}$$

$$D_3 = \frac{1}{1 - \left(\frac{e^{-1.59s}}{\lambda_{f,3}s + 1}\right)}$$

Acknowledgment

This work is supported in part by National Natural Science Foundation of China (No. 60474031), Science and Technology Rising-Star program of Shanghai (04QMH1405), and Hong Kong RGC (612906).

Literature Cited

(1) Ogunnaike, B. A.; Ray, W. H. *Process Dynamics, Modelling and Control*; Oxford University Press: Oxford, U.K., 1994.

(2) Seborg, D. E.; Edgar, T. F.; Mellichamp, D. A. *Process Dynamic and Control*, 2nd Edition; Wiley: Hoboken, NJ, 2004.

(3) Wang, Y. G.; Cai, W. J.; Ge, M. Decentralized relay-based multivariable process identification in the frequency domain. *IEEE Trans. Autom. Control* **2003**, *48* (5), 872−877.

(4) Wang, Q. G.; Zou, B.; Lee, T. H. Auto-tuning of multivariable PID controllers from decentralized relay feedback. *Automatica* **1997**, *33* (3), 319−330.

(5) Halevi, Y.; Palmor, Z. J.; Efrati, T. Automatic tuning of decentralized PID controllers for MIMO processes. *J. Process Control* **1997**, *7* (2), 119−128.

(6) Choi, J. Y.; Lee, J.; Jung, J. H. Sequential loop identification of multivariable process models. *Comput. Chem. Eng.* **2000**, *24* (2), 809−814.

(7) Toh, W. H.; Rangaiah, G. P. A Methodology for Autotuning of Multivariable Systems. *Ind. Eng. Chem. Res.* **2002**, *41* (18), 4605−4615.

(8) Shiu, S. J.; Hwang, S. H. Sequential Design Method for Multivariable Decoupling and Multiloop PID Controllers. *Ind. Eng. Chem. Res.* **1998**, *37* (1), 107−119.

(9) Shen, S. H.; Yu, C. C. Use of relay-feedback test for automatic tuning of multivariable systems. *AIChE J.* **1994**, *40* (4), 627−646.

(10) Loh, A. P.; Vasnani, V. U. Describing function matrix for multivariable systems and its use in multiloop PI design. *J. Process Control* **1994**, *4* (3), 115−120.

(11) Holt, B. R.; Morari, M. Design of resilient processing plants—VI. The effect of right-half-plane zeros on dynamic resilience. *Chem. Eng. Sci.* **1985**, *40* (1), 59−74.

(12) Holt, B. R.; Morari, M. Design of resilient processing plants—V. The effect of deadtime on dynamic resilience. *Chem. Eng. Sci.* **1985**, *40* (7), 1229−1237.

(13) Havre, K.; Skogestad, S. Effect of RHP zeros and poles on the sensitivity functions in multivariable systems. *J. Process Control* **1998**, *8* (3), 155−164.

(14) Morari, M.; Zafiriou, E. *Robust Process Control*; Prentice Hall: Englewood Cliffs, NJ, 1989.

(15) Skogestad, S.; Postlethwaite, I. *Multivariable Feedback Control: Analysis and Design*, 2nd Edition; Wiley: Chichester, U.K., 2005.

(16) Zhou, K. M.; Doyle, J. C.; Glover, K. *Essentials of Robust Control*; Prentice Hall: Englewood Cliffs, NJ, 1998.

(17) Jerome, N. F.; Ray, W. H. Model-predictive control of linear multivariable systems having time delays and right-half-plane zeros. *Chem. Eng. Sci.* **1992**, *47* (4), 763−785.

(18) Wang, Q. G.; Zhang, Y.; Chiu, M. S. Decoupling internal model control for multivariable systems with multiple time delays. *Chem. Eng. Sci.* **2002**, *57* (1), 115−124.

(19) Liu, T.; Zhang, W. D.; Gu, D. Y. Analytical Design of Decoupling Internal Model Control (IMC) Scheme for Two-Input−Two-Output (TITO) Processes with Time Delays. *Ind. Eng. Chem. Res.* **2006**, *45* (9), 3149−3160.

(20) Alevisakis, G.; Seborg, D. E. An extension of the Smith Predictor to multivariable linear systems containing time delays. *Int. J. Control* **1973**, *3* (17), 541−557.

(21) Wang, Q. G.; Zou, B.; Zhang, Y. Decoupling Smith predictor design for multivariable systems with multiple time delays. *Chem. Eng. Res. Des. Trans. Inst. Chem. Eng., Part A* **2000**, *78* (4), 565−572.

(22) Desbiens, A.; Pomerleau, A.; Hodouin, D. Frequency based tuning of SISO controllers for two-by-two processes. *IET Control Theory Appl.* **1996**, *143* (1), 49−56.

(23) Wang, Q. G.; Zhang, Y.; Chiu, M. S. Non-interacting control design for multivariable industrial processes. *J. Process Control* **2003**, *13* (3), 253−265.

(24) Liu, T.; Zhang, W. D.; Gao, F. Analytical decoupling control strategy using a unity feedback control structure for MIMO processes with time delays. *J. Process Control* **2007**, *17* (2), 173−186.

(25) Waller, M.; Waller, J. B.; Waller, K. V. Decoupling Revisited. *Ind. Eng. Chem. Res.* **2003**, *42* (20), 4575−4577.

(26) Wang, Q. G.; Huang, B.; Guo, X. Auto-tuning of TITO decoupling controllers from step tests. *ISA Trans.* **2000**, *39* (4), 407−418.

(27) Perng, M. H.; Ju, J. S. Optimally decoupled robust control MIMO plants with multiple delays. *IET Control Theory Appl.* **1994**, *141* (1), 49−56.

(28) Lee, J.; Kim, D. H.; Edgar, T. F. Static Decouplers for Control of Multivariable Processes. *AIChE J.* **2005**, *51* (10), 2712−2720.

(29) Åström, K. J.; Johansson, K. H.; Wang, Q. G. Design of decoupled PI controllers for two-by-two systems. *IET Control Theory Appl.* **2002**, *149* (1), 74−81.

(30) Pomerleau, D.; Pomerleau, A. Guide lines for the tuning and the evaluation of decentralized and decoupling controllers for processes with recirculation. *ISA Trans.* **2001**, *40* (4), 341−351

(31) Liu, T.; Zhang, W.; Gu, D. Analytical Multiloop PI/PID Controller Design for Two-by-Two Processes with Time Delays. *Ind. Eng. Chem. Res.* **2005**, *44* (6), 1832−1841.

(32) Chen, D.; Seborg, D. E. Design of decentralized PI control systems based on Nyquist stability analysis. *J. Process Control* **2003**, *13* (1), 27−39.

(33) Zhang, Y.; Wang, Q. G.; Åström, K. J. Dominant pole placement for multi-loop control systems. *Automatica* **2002**, *38* (7), 1213−1220.

(34) Lee, T. K.; Shen, J.; Chiu, M. S. Independent design of partially decentralized controllers. *J. Process Control* **2001**, *11* (4), 419−428.

(35) Lundström, P.; Skogestad, S. Two-degree-of-freedom controller design for an ill-conditioned distillation process using μ-synthesis. *IEEE Trans. Autom. Control* **1999**, *7* (1), 12−21.

(36) Prempain, E.; Bergeon, B. A multivariable two-degree-of-freedom control methodology. *Automatica* **1998**, *34* (12), 1601−1606.

(37) Limebeer, D. J. N.; Kasenally, E. M.; Perkins, J. D. On the design of robust two degree of freedom controllers. *Automatica* **1993**, *29* (1), 157−168.

(38) Huang, H. P.; Lin, F. Y. Decoupling Multivariable Control with Two Degrees of Freedom. *Ind. Eng. Chem. Res.* **2006**, *45* (9), 3161−3173.

(39) Jerome, N. F.; Ray, W. H. High-performance multivariable control strategies for systems having time delays. *AIChE J.* **1986**, *32* (6), 914−931.

Received for review October 10, 2006
Revised manuscript received April 25, 2007
Accepted July 30, 2007

IE0612921